Energetics and kinetics of a conformational switch in G-quadruplex DNA

Published in final edited form as:
J Phys Chem B. 2009 March 5; 113(9): 2676–2683.

Energetics and kinetics of a conformational switch in G-quadruplex DNA

Robert D. Gray, **Jing Li**, and **Jonathan B. Chaires***
James Graham Brown Cancer Center University of Louisville 529 S. Jackson St. Louisville, KY 40202 USA

Abstract

Circular dichroism and differential scanning calorimetry were used to determine the energetics of the conformational switch of the human telomere quadruplex formed by the sequence d[AGGG $(TTAGGG)_3$] between the sodium basket form and the potassium hybrid form. The energy barrier separating the two conformations was found to be modest, only 1.4−2.4 kcal mol^{-1}. The kinetics of exchange of bound K^+ for Na^+ cations and the concomitant conformational switch was assessed by measuring time-dependent changes in the circular dichroism spectrum accompanying the cation exchange reaction. The time course of these changes was found to consist of three distinct kinetic processes: a rapid phase that was complete in less than 5 ms followed by two slower phases with relaxation times of 40−50 s and 600−800 s at 25 °C and pH 7.0. We interpret these kinetics in terms of a model in which the bound Na^+ cations are rapidly replaced by K^+ followed by relatively slow structural rearrangements to generate the final K^+-bound product(s). Circular dichroism studies showed that addition of the porphyrin TmPyP4 promoted conversion of the basket to the hybrid form. The kinetics of the TmPyP4-induced conformational change were the same as those observed for the cation exchange reaction.

DNA is allosteric [1-4]. DNA binding interactions can be coupled to either long-range or local conformational transitions in the nucleic acid. Preferential binding to one DNA conformational form over another provides the thermodynamic driving force for the allosteric conversion to the preferred structural form [5]. Examples abound, and have been reviewed by Schurr and coworkers [3]. One particularly well-characterized example is the allosteric conversion of left-handed Z-DNA to a right-handed conformation by a variety of small molecule intercalators [6-10]. In one case, an enantiomeric pair of the anthracycline daunorubicin was synthesized [8]. One enantiomer of daunorubicin converted Z DNA to a right-handed form by virtue of preferential binding to B-DNA. In contrast, the other enantiomer bound preferentially to Z-DNA, and converted B-DNA to a left-handed form. Against this larger background, it is hardly surprising that small molecules can act as “drivers” or “switches” to facilitate the folding of, or to alter the conformation of, G-quadruplex DNA. The purpose of this work is to describe in quantitative detail the kinetics and equilibria of a conformational transition in a G-quadruplex that might give rise to allosteric interactions.

Four guanine bases can hydrogen bond with one another to form a planar G-quartet, the key structural element in G-quadruplex DNA [11]. G-quadruplex DNA can form either inter- or intra-molecularly, and features stacked G-quartets linked by a variety of loop arrangements and strand orientations. The diversity of G-quadruplex structures has been recently reviewed [12-14]. The energetic and kinetic aspects of the formation of G-quadruplex structures were reviewed recently[15]. We focus here on a conformational transition of the G-quadruplex formed

*__Corresponding author__: *Telephone*: 502 852 1172; *Email*: j.chaires@louisville.edu.

by the human telomere sequence 5'-AGGG(TTAGGG)$_3$. This sequence was shown by NMR to fold into an antiparallel "basket" form in the presence of Na^+ [16]. The basket structure features three stacked G-quartets linked by two lateral and one diagonal loops. A crystal structure was subsequently reported in which the identical sequence adopted an unusual, highly symmetric "propeller" structure in the presence of K^+ [17]. In this propeller structure, three stacked G-quartets were linked by three double chain-reversal side loops, producing strand segments that were in a parallel arrangement within the stacked quartets. Biophysical studies showed that this crystal structure was not the predominant form in solution [18]. Subsequent circular dichroism and NMR studies using slight modifications of the above human telomere sequence confirmed and extended the biophysical studies and showed that in K^+ solutions a "hybrid" structure was formed [19-22]. The hybrid structure features an antiparallel strand arrangement, two lateral loops, and one side chain-reversal loop. The cahin-reversal side loop can be the first loop near the 5' end ("hybrid 1") or the last loop nearest the 3' end ("hybrid 2"). Figure 1 shows some of the structures adopted by the human telomere sequence in solution.

Soon after possible biological roles for G-quadruplexes were discovered, it was recognized that specific cations could "switch" quadruplex conformations, and it was proposed that such a switching mechanism could have functional utility [23]. The phenomena of cation-controlled conformational switching of quadruplexes has been insightfully reviewed by Hud and coworkers [24,25].

The literature on ligand-induced conformational switching is less extensive. Arthanari and Bolton showed that porphyrins can "catalyze" the interconversion of uniand bimolecular folded antiparallel quadruplex structures to parallel-stranded "G-wire" structures [26]. The process is certainly not catalysis, since the porphyrin is not released and recycled, but remains bound to parallel-stranded quadruplex structures. Hurley and coworkers showed that the perylene derivative PIPER can act as a "driver" to accelerate the assembly of an oligonucleotide containing two tandem repeats of the human telomere sequence TTAGGG into bi- and tetramolecular structures[27]. A naphthyridine dimer was shown to convert the Na^+ basket form of the human telomere quadruplex to an unknown conformation but with a circular dichroism spectrum characteristic of a parallel or "G-wire" structure [28]. Diseleno sapphyrin was reported to convert the basket quadruplex form to a hybrid form [29]. An anthracene derivative was shown to promote folding of the single-stranded human telomere sequence into a parallel quadruplex structure in the absence of cations, and further to convert a preformed Na^+ basket quadruplex structure into the parallel form [30]. While it was supposed in that study that the parallel form corresponded to the crystalline "propeller" conformation, no evidence was provided to eliminate the possibility that "G-wires" formed instead. Monchaud and coworkers described a remarkable metallo ligand whose affinity for quadruplex structures could be modulated by a metal-mediated switch in ligand conformation. The ligand could switch the quadruplex hybrid form to the basket conformation, and facilitated folding of single strands into the basket conformation. One enantiomer of a chiral metallo-supramolecular complex was recently found to selectively bind to the hybrid quadruplex form, and to convert the basket form to that conformation[31]. The porphyrin TmPyP4 was reported to induce folding of single strands into a basket conformation in the absence of cations, or to convert the hybrid form in K^+ to the basket form [32].

In all of the above cases, ligand binding must be thermodynamically coupled to G-quadruplex folding or conformational equilibria. Full understanding of such coupling requires understanding of the conformational equilibria of the G-quadruplex. The purpose of this work is to describe the energetics and kinetics of one such conformational transition, the K^+ induced switch from the basket to the hybrid form. In addition, we show that the porphyrin TmPyP4 can switch the basket form to the hybrid form, and show the possible energy balance for the process.

Materials & Methods

Materials

The oligonucleotide 5'-AGGG(TTAGGG)$_3$ was purchased from Integrated DNA Technologies, Inc., (Coralville, IA) and was used without further purification. Tetrabutyl ammonium phosphate, NaCl, KCl and TmPyP4 were from Sigma. All equilibrium studies were done in filtered BPES and BPEK buffers, which consisted of 6 mM Na_2HPO_4, 2 mM NaH_2PO_4, 1 mM Na_2EDTA, 185 mM NaCl or KCl (respectively) at pH 7. The oligonucleotide was dissolved in buffer overnight and was then heated in a water bath until the temperature reached 95 °C. The samples were allowed to equilibrate for 10 minutes at 95 °C, then were slow cooled to room temperature overnight in the water bath. The samples were stored at 4° C. An extinction coefficient of 198,450 ± 2,790 $M^{-1}cm^{-1}$ at 260 nm was used to calculated the concentration of the *folded* quadruplex. For the unstructured single-stranded form, an extinction coefficient of 228,500 $M^{-1}cm^{-1}$ at 260 nm was used. Kinetic studies were carried out in 10 mM tetrabutylammonium phosphate, 1 mM EDTA, pH 7.00, the same conditions as used for our previous kinetic investigation of the folding of this oligonucleotide [33].

Circular Dichroism

Circular dichroism experiments were performed on a JASCO model J-810 circular dichroism spectropolarimeter equipped with a Peltier temperature controller. Equilibrium CD experiments were performed on samples with A_{260} of ~0.8. The measurements were made at 20°C, using a 3 ml square quartz cuvette with a 1 cm path length. CD spectra were recorded from 220 nm to 340 nm with the following parameters: scanning speed of 100 nm/min; band width of 1 nm; response of 1 sec; data interval of 0.2 nm; and a total of 4 accumulations. The buffer spectrum was subtracted from the sample spectrum for each experiment. Origin software (ver.7.0 from OriginLab Corp. Northampton, MA) was used to graph data. For studies in which the mole fraction of Na^+ was varied, a series of solutions were prepared by mixing appropriate volumes of BPES and BPEK to span the range of 0 − 1.0 mole fraction. A solution containing concentrated quadruplex stock solution was added to each solution over the mole fraction span, and allowed to equilibrate for 24 hours prior to CD measurements. In experiments with TmPyP4, no attempt was made to subtract possible contributions to the CD from the ligand because of possible induced CD effects from the ligand.

Differential Scanning Calorimetry

DSC experiments were done using a Calorimetric Sciences, Inc. (Spanish Fork, Utah) NanoDSC instrument. Sample concentrations for DSC studies were 189 μM (in strands). Scan rates of 1 °C min^{-1} were used in all cases. Buffer versus buffer baseline scans were determined and subtracted from denaturation scans prior to normalization and analysis.

Kinetics

CD kinetic experiments were carried out either in single wavelength mode at 291 or 261 nm or in “interval scan mode”. Spectra were measured in a 1-cm pathlength cuvette thermostatted at 25.0 °C with an oligonucleotide concentration of approximately 7 μM [33]. The spectral data were corrected for dilution by applying a correction factor (generally <2%). NaCl, KCl or TmPyP4 were added manually from concentrated stock solutions with mixing provided by an in-cuvette magnetic stirring bar. Recording time-dependent spectral changes was initiated within 4−5 s after reagent addition. Changes in UV absorption were also assessed by multi-wavelength stopped flow spectrophotometry as previously described [33].

Analysis of kinetic data

Single-wavelength progress curves were analyzed by nonlinear least squares using the single or multi-exponential fitting function of the Origin 7.0 package as appropriate.

Multi-wavelength kinetic data sets consist of a matrix $\boldsymbol{\theta_{i,j}}$ where the element $\theta_{i,j}$ equals the ellipticity determined at wavelength i and time j. These $\boldsymbol{\theta_{i,j}}$ matrices contain 26 wavelength readings from 255 to 305 nm spaced by 2 nm and 60 time points spaced by 19 s. They were analyzed by the method of singular value decomposition (SVD) to define the minimum number of spectroscopic species, the basis spectra for these species, and the concentration-time profiles of the species [34-37]. The $\boldsymbol{\theta_{i,j}}$ matrices were fit by non-linear least squares analysis to single or multiple exponentials (Eq 1) to allow determination of the absolute spectra of the kinetically significant species and the rate constants for their formation and decay:

$$\theta_{t,\lambda}=\theta_{\infty,\lambda}+\theta_{1,\lambda}\cdot\exp(-k_1 t)+\theta_{2,\lambda}\cdot\exp(-k_2 t) \quad (1)$$

where $\theta_{t,\lambda}$ is the value of the ellipticity at time t, $\theta_{\infty,\lambda}$ is the final value of θ, $\theta_{1,\lambda}$ and $\theta_{2,\lambda}$ are amplitude factors for the first and second exponentials at wavelength λ, respectively and k_1 and k_2 are the rate constants. The program Specfit/32 version 3.0 (Spectrum Software Associates, Marlborough, MA) was used for the SVD analysis as well as for fitting the progress curves.

Results and Analysis

Thermodynamics of the conformational switch

Figure 2A shows primary CD spectra as a function of the mole fraction sodium. The spectra shift from one with a positive maximum near 295 nm and a negative minimum near 260 nm at a mole fraction of 1.0 to a spectrum with a positive maximum near 290 nm at a mole fraction of 0. There are apparent isoselliptic points near 250 and 302 nm. Figure 2B shows the molar ellipticity at 265 nm plotted as a function of mole fraction sodium. The data are fit to a sigmoidal curve with a midpoint of 0.877 mole fraction, and upper and lower limiting values of molar ellipticity of 96,837 and −350,920, respectively.

The presence of two well-defined isoselliptic points in figure 2A suggest (but do not prove) that the transition between the sodium and potassium quadruplex forms is a two-state process without any significantly populated intermediate species. The assumption that the transition is two-state was validated more rigorously by the use of singular value decomposition (SVD) analysis [34,36,37], as shown in Supplementary Information. SVD shows conclusively that there are only two major spectral species that combine linearly to produce the family of spectra shown in figure 2A, and that for further analysis of the data the use of the two-state assumption is justified. The CD data in Figure 2A can be used to calculate the fraction of the conformational forms at each mole fraction. The fraction of the potassium form f is given by the equation:

$$f=\frac{\varepsilon-\varepsilon_L}{\varepsilon_U-\varepsilon_L} \quad (2)$$

In eq. 2, ε is the ellipticity at a given mole fraction, and ε_U and ε_L are the upper and lower limiting values of the ellipticity given above. Values of f can be used to calculate the dimensionless equilibrium constant at each mole fraction:

$$K = \frac{f}{1 - f} \tag{3}$$

K refers to the transition from the sodium form to the potassium form. From K, the free energy change can be calculated from the standard Gibbs equation

$$\Delta G^{0}_{Na \to K} = - RT \ln K \tag{4}$$

where R and T are the gas constant and temperature, respectively. Figure 3 shows calculated free energy changes as a function of mole fraction sodium. A linear fit of the data allows extrapolation to 1.0 mole fraction sodium, yielding a value of 1.4 ± 0.3 kcal mol^{-1}. This value represents the energy barrier for converting the basket form to the hybrid form in a sodium solution.

The free energy barrier between the quadruplex conformational forms may also be calculated from DSC data. Figure 4 show thermograms for the thermal denaturation of the sodium basket form and the potassium hybrid forms. These thermograms yield the enthalpy (ΔH) and entropy (ΔS) values for the denaturation reaction through the equations

$$\begin{aligned} \Delta H &= \int C_p dT \\ \Delta S &= \int \frac{C_p}{T} dT \end{aligned} \tag{5}$$

where C_p is the excess heat capacity change and T is the temperature. The thermograms in figure 4 yield values of ΔH = 37.1 kcal mol^{-1} and ΔS=0.110 kcal mol^{-1} deg^{-1} for the sodium form. For the potassium form, ΔH = 49.2 kcal mol^{-1} and ΔS=0.143 kcal mol^{-1} deg^{-1} were obtained. From triplicate determinations, the error in enthalpy and entropy values is ~5%. From the ΔH and ΔS values, the free energy change can be calculated, as shown in Figure 5, from the equation

$$\Delta G = \Delta H - T \Delta S \tag{6}$$

This treatment assumes that the heat capacity change for the folded and unfolded forms is zero, an assumption that can be justified by the lack of a detectable shift in the preand post-transition baselines in the data in figure 4. (The assumption that $\Delta C_p = 0$ is subject to debate [38]). Once free energy values are calculated for the denaturation reactions, the free energy for conversion from the sodium to the potassium form can be calculated using the free energy cycle shown as an inset in Figure 5. Assuming that the denatured, single-stranded state is the same in sodium or potassium,

$$\Delta G_{III} = \Delta G_{II} - \Delta G_{I} \tag{7}$$

At 25°C, a value of ΔG_{III}= 2.4 ± 0.3 kcal mol^{-1} is estimated. This value is in fair agreement with the value calculated from the CD spectral data. Together, the data suggest that the energy barrier for the conversion from the basket form to the hybrid form is modest, only 1.4 − 2.4 kcal mol^{-1}.

Kinetics of the conformational switch

Figure 6 shows progress curves for $Na^+ \rightarrow K^+$ exchange measured by CD at 291 nm and 261 nm. The black traces represent the ellipticity of the basket form in 30 mM NaCl during the time period immediately preceding addition of KCl. The red traces show the changes in ellipticity subsequent to KCl addition. Comparison of starting ellipticities (represented by the black traces for the Na^+ state at 291 and 261 nm) reveals that a large increase in CD signal occurred during the ~5 s mixing dead time. For example, at 291 nm, θ increased from ~13 mdeg to >23 mdeg while at 261 nm, θ increased from −18.5 mdeg to > −7.5 mdeg. At both wavelengths, the rapid increase in ellipticity was followed by smaller biphasic changes. At 291 nm, the more rapid decrease in ellipticity was followed by a smaller increase in ellipticity. At 261 nm, the ellipticity increased in both the rapid and slower phases. Stopped flow mixing experiments monitoring changes in the UV absorption spectrum of the Na^+-form on mixing with KCl showed very rapid changes in absorbance that were complete within the ~5 ms dead time of the apparatus. These rapid changes in absorbance probably correspond to the rapid changes in ellipticity that occurred in the dead time of the CD experiments. In addition, slower biphasic changes in UV absorption were observed with approximately the same relaxation times as those in the CD experiments (data not shown).

The stopped flow experiments therefore show that the initial most rapid spectroscopic changes occur more rapidly than measurable by this method and therefore are completed in less than ~5 ms. The progress curves for Na/K exchange in Fig. 6 are therefore compatible with a three-step pathway shown in Scheme 1:

$$\mathrm{Na} \rightarrow \mathrm{I1} \leftrightarrow \mathrm{I2} \leftrightarrow \mathrm{K} \qquad \text{(Scheme 1)}$$

where Na and K represent the Na^+- and K^+-bound states of the oligonucleotide and I1 and I2 represent intermediate states. The conversion of the Na state to intermediate I1 occurs within <5 ms, while the I1 ↔ I2 ↔ K sequence is described by two slower bi-exponential processes with k_1 and k_2 as apparent rate constants for steps I1 ↔ I2 and I2 ↔ K, respectively.

We utilized multi-wavelength kinetic CD spectroscopy coupled with SVD analysis of the kinetic data matrices to confirm that the observed changes in CD spectrum over the full range of observable wavelengths conform to the bi-exponential kinetics predicted by the sequence I1 ↔ I2 ↔ K. The results of a representative multi-wavelength kinetic experiment are shown in Figure 7. As expected from the single wavelength experiments, biphasic changes occurring over a time period of about 1100 s were observed at multiple wavelengths between 255 and 305 nm.

Analysis of the wavelength-time data matrix associated with Figure 7 by SVD (results shown in the Supplementary Information) clearly shows that three spectroscopically distinct species are required to account for the full range of ellipticity changes during the time period during which the reaction could be observed (e.g. from ~4 s after mixing until the final observation at ~1100 s). Fitting the data matrix of Figure 7 to the integrated rate equations for Scheme 1 allowed us to obtain CD spectra of species I1 and I2. Figure 8 compares the calculated CD spectra of the intermediates and final K^+-bound product with the experimental spectra of the initial Na^+ complex measured immediately prior to KCl addition. In addition, the CD spectrum of the final K^+ complex measured at the completion of the exchange reaction is shown. These spectra show that the CD spectrum of the Na^+ complex (depicted in magenta) changes rapidly (within ~5 s or less) to the spectrum of intermediate I1 (black), which then changes to that of intermediate I2 (red). This is followed by relaxation to the final K^+ species C (green). Note the close similarity between the spectrum of C determined from the kinetic data matrix and the measured equilibrium spectrum of the KCl complex (blue spectrum). This similarity shows

that the kinetic experiments completely account for the changes in CD that occur upon switching from the Na conformation to the K conformation. For the experiment shown, the rate constants for conversion of I1 to I2 and I2 to the final structure yield relaxation times τ of 44 s and 580 s, respectively, for the two steps. The variation in these values over several similar experiments is ~± 10%.

We conclude from these experiments that the conformational change from the basket to the hybrid structure induced by displacement of bound Na^+ by K^+ proceeds through two spectroscopically distinguishable intermediates.

Conformational switch induced by TmPyP4

Figure 9 shows the effects of addition of the porphyrin TmPyP4 on the conformation of quadruplex structures as monitored by circular dichroism. In Figure 9A, TmPyP4 is added to a quadruplex in Na^+ buffer that favors the basket form. The ligand induces changes in the CD spectrum similar to the changes seen in Figure 2A, suggestive of a conformational transition toward a hybrid form, although insufficient ligand was added to drive the transition to completion. In Figure 9C, the ligand is added to quadruplex in a K^+ buffer that initially favors the hybrid form. The changes observed in the CD spectra suggest slight structural alterations to the hybrid form upon ligand binding. Figure 9B shows the effect of ligand addition on quadruplex structures in a solution with mole fraction Na^+ of 0.84. Under these conditions, an equilibrium mixture of basket and hybrid forms exist, and the system is poised to be perturbed toward the conformational form most preferred by TmPyP4. The CD changes observed suggest that the preferred form is the hybrid conformation. The last spectrum in the titrations is superimposable on the last spectrum of the titration in panel C, suggesting that the ligand drove the system from one with a nearly equimolar distribution of conformational forms to one containing all ligated hybrid structures.

The porphyrin derivative TmPyP4 thus appears to act as an allosteric effector of the basket-hybrid conformational equilibrium by binding preferentially to the hybrid state. To confirm that the conformational switch occurs with similar kinetics as that induced by K^+ binding, we added a saturating amount of TmPyP4 under conditions where a mixture of the basket and hybrid species exist (e.g. $[Na^+]/([Na^+]+[K^+]) \approx 0.8$). The kinetics of the switch was determined at 291 nm (Figure 10). As with the switch triggered by K^+ binding, the relaxation to the hybrid structure initiated by porphyrin binding was characterized by three phases: a rapid step that occurred within the 4−5 s dead time, an intermediate step with a relaxation time of ~56 s, and a slow step with a relaxation time of ~740 s.

The apparent affinity of TmPyP4 for the basket and hybrid quadruplex forms was studied by equilibrium dialysis. Triplicate 1 mL samples of 25 μM (strand) quadruplex in either BPES or BPEK buffer were dialyzed against 100 mL of a 1 μM solution of TmPyP4 in matched buffer. A 3500 MWCO membrane was used. After a 24 hour equilibration period at room temperature, the distribution of free and bound ligand was determined as described previously [39,40]. Average apparent binding constants of 2.8×10^5 M^{-1} and 2.9×10^8 M^{-1} were found for binding to the basket and hybrid conformational forms, respectively. These correspond to binding free energies of −7.4 and −11.5 kcal mol^{-1} to the respective conformations. This experimental approach was designed to avoid allosteric binding by maintaining the concentrations of basket or hybrid conformations in large excess to the free ligand. The stoichiometric ratio of ligand is insufficient to drive the conformational transition from the basket to the hybrid form. The challenging task of the determination of more complete allosteric binding isotherms is beyond the scope of this work, but will be the subject of a future communication.

Discussion

Equilibrium studies show that the potassium-induced switch of the human telomere quadruplex from the basket to the hybrid conformation is a two-state process with only a modest energy barrier of 1.4 − 2.4 kcal mol^{-1}. Given the small energy difference between the two conformations, it should be fairly easy for small molecules or proteins to drive the conformation equilibrium toward the form with their preferred binding site.

The kinetic studies reported here reveal that the exchange of Na^+ cations for K^+ cations proceeds by a complex series of reactions as indicated by the multiphasic kinetic CD profile. The changes in the CD spectrum indicate at least three kinetic processes, suggesting a minimal pathway shown in Scheme 1. The most rapid process, which we attribute to a rapid replacement of the Na^+ cations by K^+ cations bound in the central channel of the quadruplex has been shown to occur very rapidly, on a μs to ms time scale[25,41,42]. In the experiments reported here, this exchange process evidently results in a large increase in ellipticity at both 261 and 291 nm that occurs within a dead time of 4−5 s. Subsequent CD changes, which are smaller in magnitude than the initial "burst" reaction, occur on a much slower time scale, with relaxation times in the neighborhood of 40−50 s and 600−800 s. At 291 nm, the intermediate phase is characterized by a decrease in ellipticity followed by a smaller increase. In contrast, the intermediate and slower steps at 261 nm both proceed with an increase in ellipticity. As noted above, the corresponding changes in UV absorption take place within the ~5 ms dead time of our stopped-flow device and are followed by much slower changes in UV absorption that more or less track the changes in CD. The apparent kinetic complexity can be reconciled with the simpler two-state transition found in equilibrium studies by noting that 24 hour equilibration periods were used in the latter. At equilibrium, no intermediate states are populated to any significant degree.

Based on these data, we propose that the structural changes responsible for the observed CD changes can be explained by the scheme shown in Figure 11. In step 1 (τ_1 ~250 μs) the sodium cations within the quadruplex channel are replaced by potassium ions as suggested by previous NMR experiments [42]. This cation exchange would give rise to intermediate I1, which consists of a potassium-loaded channel that retains aspects of the Na-structure, including the antiparallel basket topology and a strained arrangement of the G-quartets due to the different coordination of the Na^+ and K^+ cations. Intermediate I2 is a partially unfolded triplex structure resulting from the redirection of either segments 1 or 4 (magenta color) which rearrange to form a hybrid-1 or hybrid-2 type structure possibly with a mixture of other structures as suggested by NMR data [12]. A triplex folding intermediate for the basket to hybrid conformational change has previously been proposed by Dai et al. [12] and by Mashimo et al. [43]. Preliminary data measuring the kinetics of cation exchange in basket variants in which the adenines at positions 1, 7, 13 and 21 were separately replaced with the fluorescent analog 2-aminopurine suggests that only segment 1 undergoes a change in emission that is consistent with a major reorientation of loop 1. Thus, we suggest that the predominant new conformer formed is the hybrid-1 conformation.

The porphyrin TmPyP4 acts as an allosteric effector of quadruplex conformation, and drives a switch to the hybrid form. The driving force is the higher binding affinity for the hybrid form over the basket form. Figure 12 shows a tentative energy balance for the system. Ligand binding to the hybrid form is ~4 kcal mol^{-1} more favorable than to the basket form. This free energy difference is sufficient to overcome the 1.4−2.4 kcal mol^{-1} cost of the basket to hybrid conversion, leaving a favorable coupling free energy[44] of about −2 kcal mol^{-1}.

Supplementary Material

Refer to Web version on PubMed Central for supplementary material.

Acknowledgments

Supported by grants CA35635 and GM077422 from the National Institutes of Health. We thank Dr. Nichola Garbett for helpful suggestions.

References

1. Hogan M, Dattagupta N, Crothers DM. Nature 1979;278:521. [PubMed: 372825]
2. Pohl FM, Jovin TM, Baehr W, Holbrook JJ. Proc. Natl. Acad. Sci. U S A 1972;69:3805. [PubMed: 4509343]
3. Schurr JM, Delrow JJ, Fujimoto BS, Benight AS. Biopolymers 1997;44:283. [PubMed: 9591480]
4. Chaires JB. ACS Chem Biol 2008;3:207. [PubMed: 18422302]
5. Dattagupta N, Hogan M, Crothers DM. Biochemistry 1980;19:5998. [PubMed: 6258628]
6. Chaires JB. Biochemistry 1985;24:7479. [PubMed: 4084594]
7. Chaires JB. J. Biol. Chem 1986;261:8899. [PubMed: 3722181]
8. Qu X, Trent JO, Fokt I, Priebe W, Chaires JB. Proc. Natl. Acad. Sci. USA 2000;97:12032. [PubMed: 11027298]
9. Walker GT, Stone MP, Krugh TR. Biochemistry 1985;24:7462. [PubMed: 4084593]
10. Walker GT, Stone MP, Krugh TR. Biochemistry 1985;24:7471. [PubMed: 2417627]
11. Gellert M, Lipsett MN, Davies DR. Proc Natl Acad Sci U S A 1962;48:2013. [PubMed: 13947099]
12. Dai J, Carver M, Yang D. Biochimie 2008;90:1172. [PubMed: 18373984]
13. Patel DJ, Phan AT, Kuryavyi V. Nucleic Acids Res 2007;35:7429. [PubMed: 17913750]
14. Burge S, Parkinson GN, Hazel P, Todd AK, Neidle S. Nucleic Acids Res 2006;34:5402. [PubMed: 17012276]
15. Lane AN, Chaires JB, Gray RD, Trent JO. Nucleic Acids Res 2008;36:5482. [PubMed: 18718931]
16. Wang Y, Patel DJ. Structure 1993;1:263. [PubMed: 8081740]
17. Parkinson GN, Lee MP, Neidle S. Nature 2002;417:876. [PubMed: 12050675]
18. Li J, Correia JJ, Wang L, Trent JO, Chaires JB. Nucleic Acids Res 2005;33:4649. [PubMed: 16106044]
19. Xu Y, Noguchi Y, Sugiyama H. Bioorg Med Chem 2006;14:5584. [PubMed: 16682210]
20. Phan AT, Kuryavyi V, Luu KN, Patel DJ. Nucleic Acids Res 2007;35:6517. [PubMed: 17895279]
21. Ambrus A, Chen D, Dai J, Bialis T, Jones RA, Yang D. Nucleic Acids Res 2006;34:2723. [PubMed: 16714449]
22. Dai J, Carver M, Punchihewa C, Jones RA, Yang D. Nucleic Acids Res 2007;35:4927. [PubMed: 17626043]
23. Sen D, Gilbert W. Nature 1990;344:410. [PubMed: 2320109]
24. Engelhart, AE.; Plavec, J.; Persil, O.; Hud, NV. Metal Ion Interactions with G-quadruplex Structures.. In: Hud, NV., editor. Nucleic Acid -Metal Ion Interactions. Royal Society of Chemistry; Cambridge: 2008. p. 114
25. Hud, NV.; Plavec, J. The Role of Cations in Determining Quadruplex Structure and Stability.. In: Neidle, S.; Balasubramanian, S., editors. Quadruplex Nucleic Acids. Royal Society of Chemistry; Cambridge: 2006. p. 100
26. Arthanari H, Bolton PH. Anticancer Drug Des 1999;14:317. [PubMed: 10625924]
27. Han H, Cliff CL, Hurley LH. Biochemistry 1999;38:6981. [PubMed: 10353809]
28. Nakatani K, Hagihara S, Sando S, Sakamoto S, Yamaguchi K, Maesawa C, Saito I. J Am Chem Soc 2003;125:662. [PubMed: 12526665]
29. Rezler EM, White E, Bashyam S, Kim M-Y, Seenisamy J, Wilson WD, Hurley LH. J. Am. Chem.l Soc 2005;127:9439.
30. Rodriguez R, Pantos GD, Goncalves DP, Sanders JK, Balasubramanian S. Angew Chem Int Ed Engl 2007;46:5405. [PubMed: 17562537]
31. Yu H, Wang X, Fu M, Ren J, Qu X. Nucleic Acids Res 2008;36:5695. [PubMed: 18776218]

32. Zhang HJ, Wang XF, Wang P, Ai XC, Zhang JP. Photochem Photobiol Sci 2008;7:948. [PubMed: 18688502]
33. Gray RD, Chaires JB. Nucleic Acids Res 2008;36:4191. [PubMed: 18567908]
34. Haq I, Chowdhry BZ, Chaires JB. Eur Biophys J 1997;26:419. [PubMed: 9404005]
35. DeSa RJ, Matheson IB. Methods Enzymol 2004;384:1. [PubMed: 15081677]
36. Hendler RW, Shrager RI. J Biochem Biophys Methods 1994;28:1. [PubMed: 8151067]
37. Henry, RW.; Hofrichter, J. Singular value decomposition: application to analysis of experimental data.. In: Brand, L.; Johnson, ML., editors. Methods in Enzymology. Vol. 210. Academic Press; New York: 1992. p. 129
38. Majhi PR, Qi J, Tang CF, Shafer RH. Biopolymers 2008;89:302. [PubMed: 18183583]
39. Ren J, Chaires JB. Biochemistry 1999;38:16067. [PubMed: 10587429]
40. Ren J, Chaires JB. Methods Enzymol 2001;340:99. [PubMed: 11494877]
41. Deng H, Braunlin WH. J Mol Biol 1996;255:476. [PubMed: 8568891]
42. Ida R, Wu G. J Am Chem Soc 2008;130:3590. [PubMed: 18293981]
43. Mashimo T, Sannohe Y, Yagi H, Sugiyama H. Nucleic Acids Symp Ser (Oxf) 2008:409.
44. Weber G. Adv Protein Chem 1975;29:1. [PubMed: 1136898]

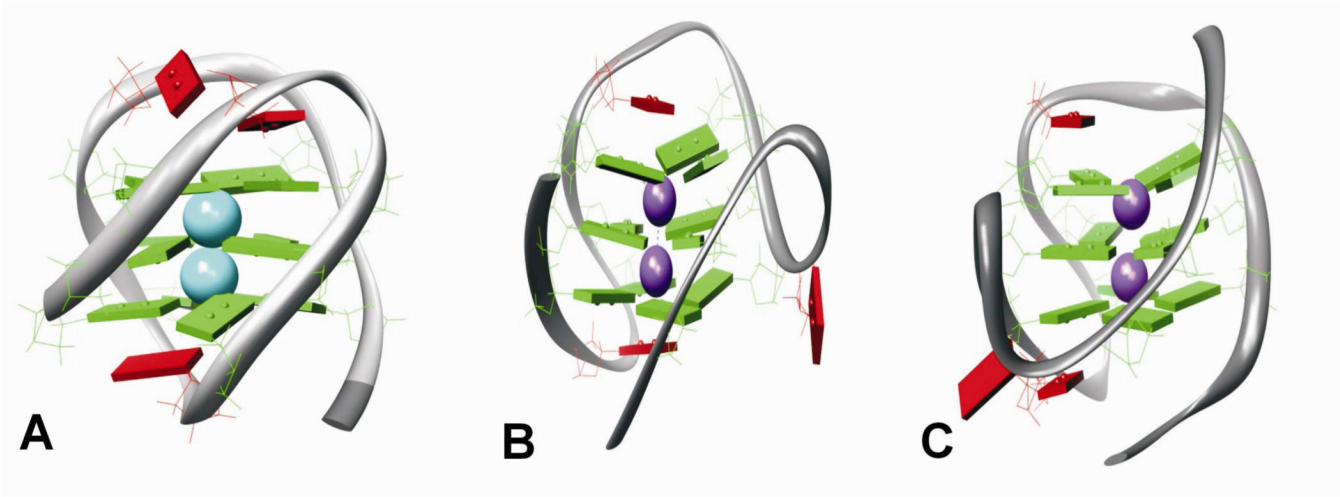

Figure 1.
Structures adopted by the sequence 5'-AGGG(TTAGGG)$_3$ in sodium and potassium solution. (A) The basket form observed in NaCl solutions. (B) “Hybrid 1” form observed in potassium solution. (C) “Hybrid 2” form observed in potassium solution.

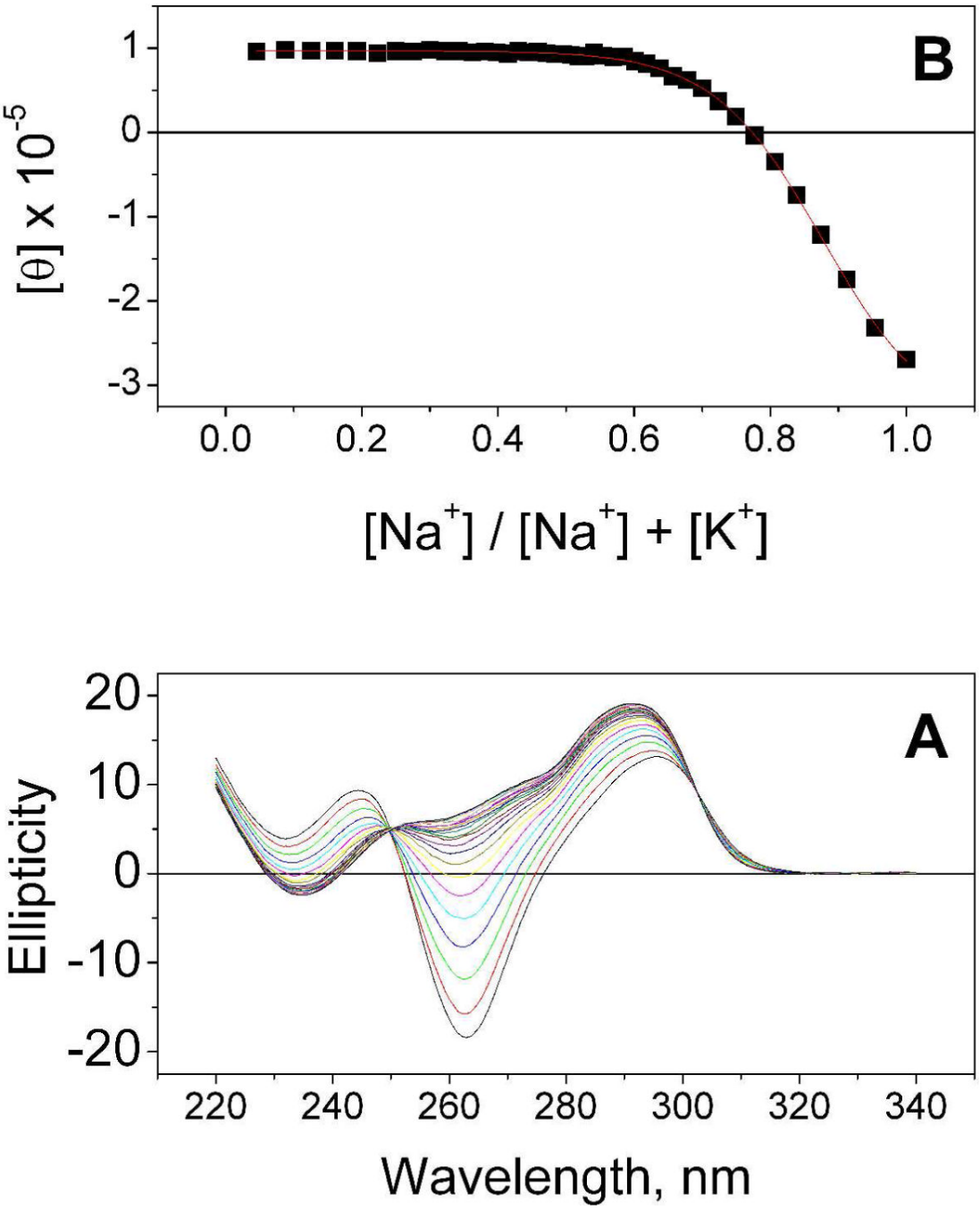

Figure 2.

CD spectra as a function of mole fraction sodium chloride. (A) Spectra are shown for mole fraction sodium ranging from 0 (top curve) to 1.0 (bottom curve). Isoseliptic points are evident at 250 and 302 nm. (B) Molar ellipticity at 265 nm (from panel A) plotted as a function of mole fraction sodium. A fit of the data to a sigmoidal function (red line) is shown, with the parameters described in the text.

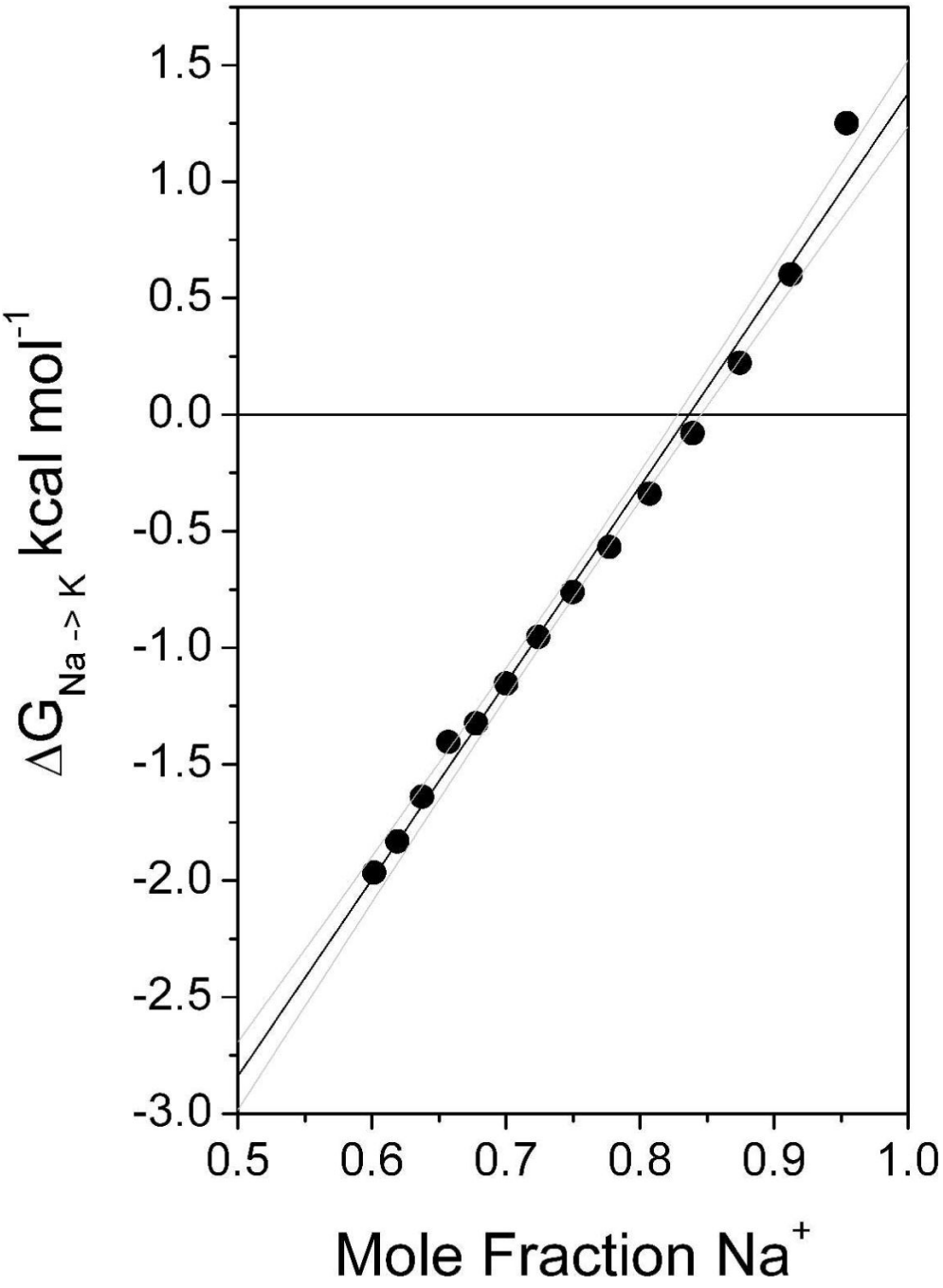

Figure 3.
Free energy for the conversion of the sodium basket form to the potassium hybrid form plotted as a function of the mole fraction sodium. The least squares linear fit to the data is shown by the solid line, along with the 95% confidence interval (gray lines).

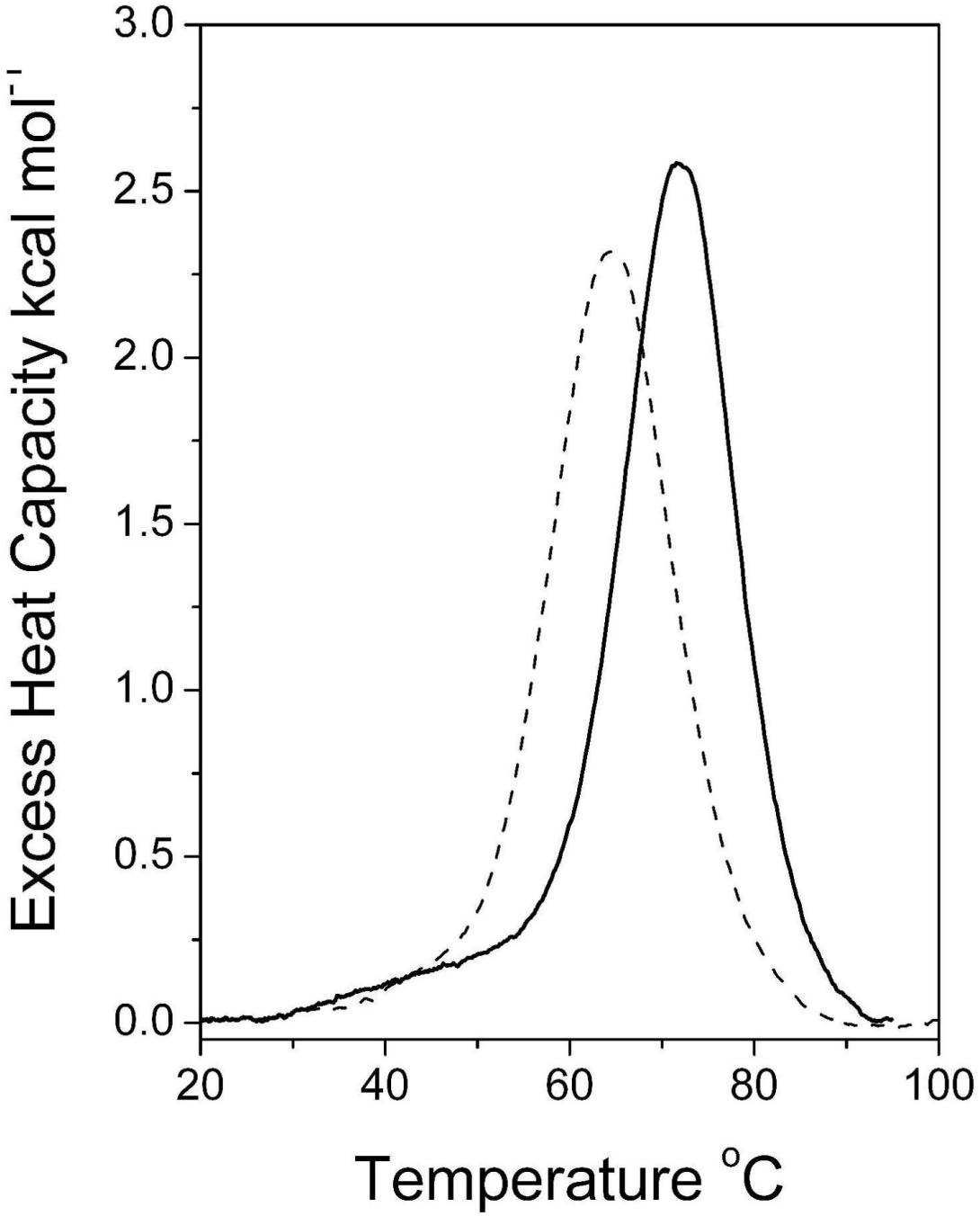

Figure 4.
DSC thermograms for the denaturation of 5'-AGGG(TTAGGG)$_3$ in BPES buffer (dashed line) and BPEK buffer (solid line).

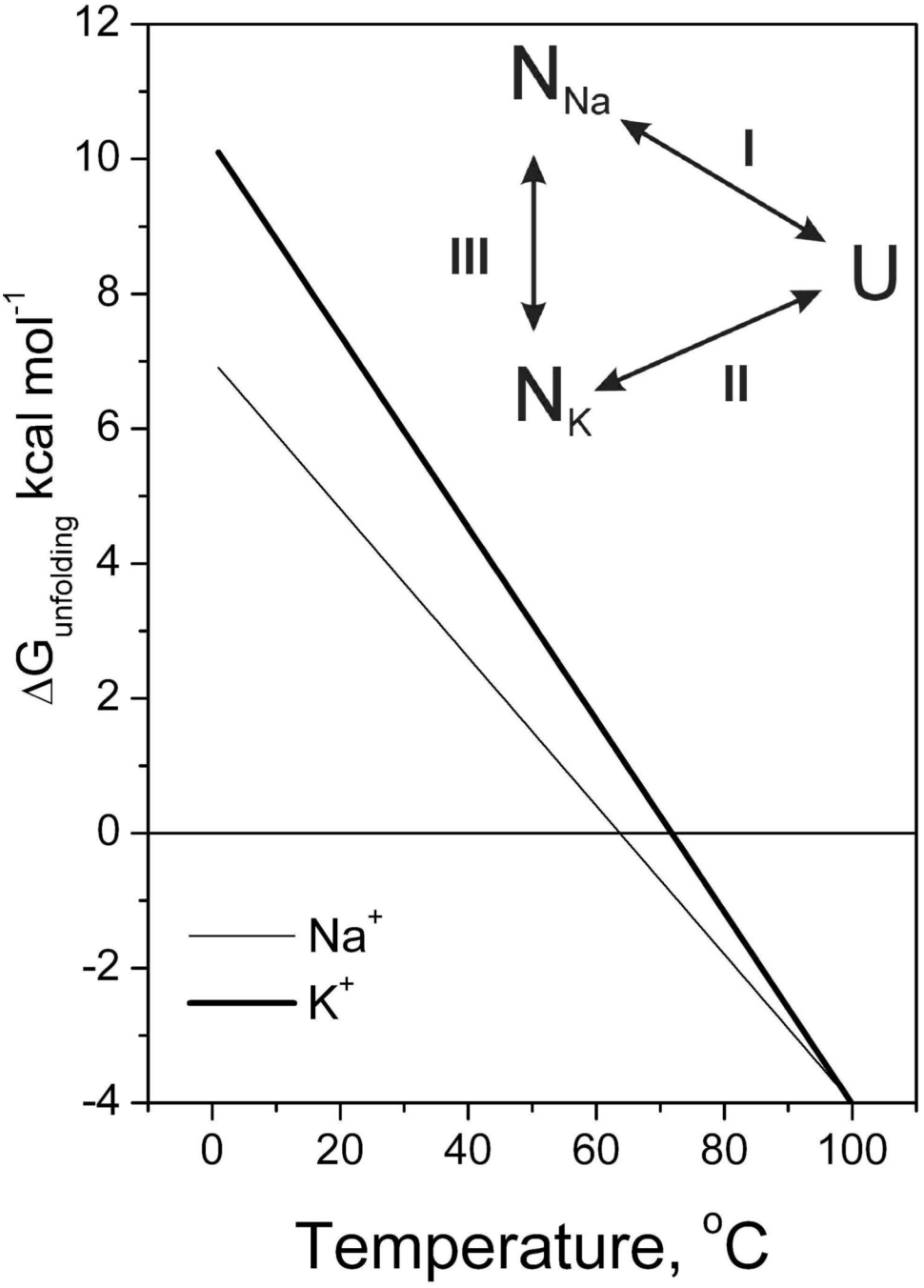

Figure 5.
Calculated free energy change for the unfolding of the human telomere quadruplex in sodium or potassium solutions. The inset shows the thermodynamic cycle that may be used to calculate the free energy difference between the sodium and potassium quadruplex forms, assuming that the denatured state (U) is identical for both forms.

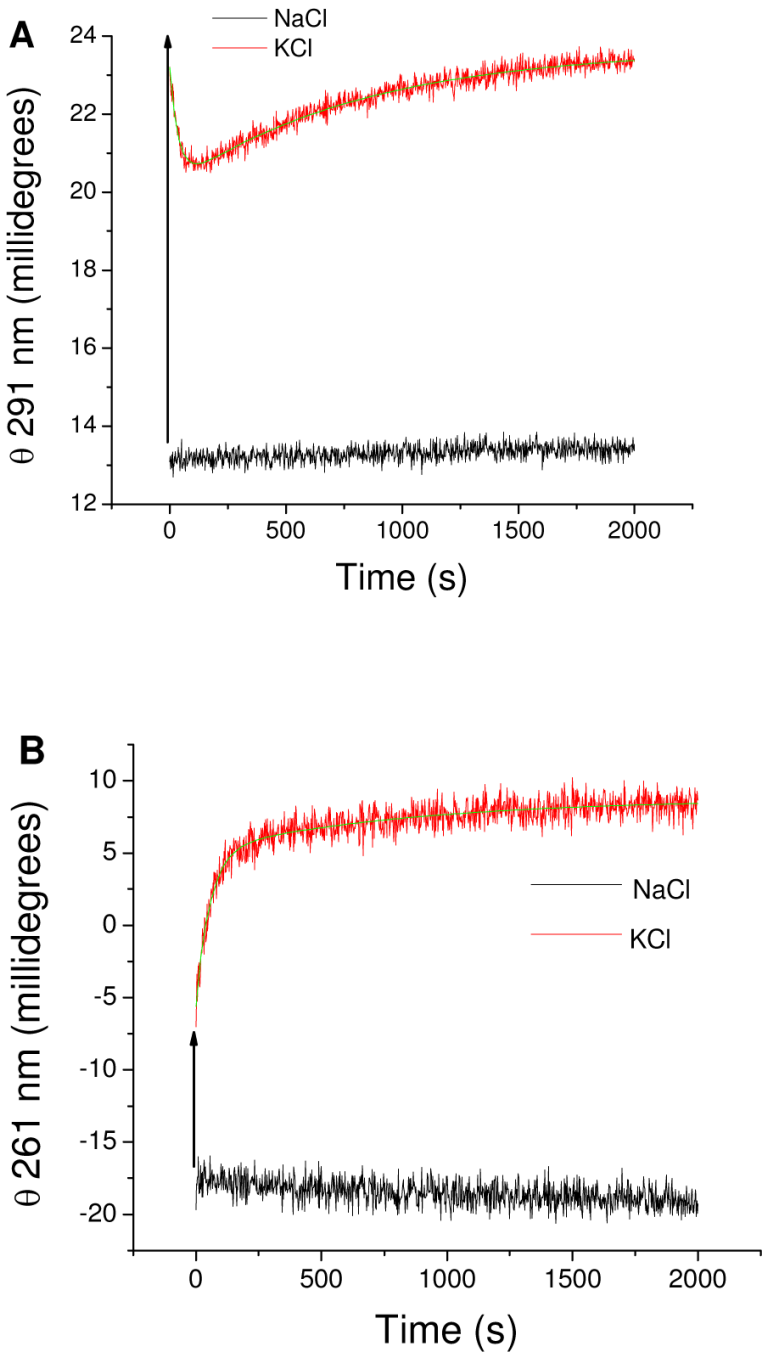

Figure 6.

Kinetics of Na^+/K^+ exchange measured by changes in CD at 291 nm (Panel A) and 261 nm (Panel B). The black lines represents the CD signal recorded in 30 mM NaCl immediately prior to the addition of KCl to trigger the conformational switch from the basket state to the hybrid state. The red lines represent progress of the change in CD signal following addition of KCl to give a final concentration of 50 mM. The data have been corrected for ~1.6% dilution resulting from the KCl addition. The vertical arrows indicated the rapid change in ellipticity that occurs during the ~ 5 s mixing time between KCl addition and initiation of data recording. The green lines show the least squares fit of each data set to two exponentials. For Panel A, the optimized relaxation times are $\tau_1 = 37.4 \pm 1.8$ s and $\tau_2 = 812 \pm 24$ s; in Panel B $\tau_1 = 55.3$

± 3.1 s and τ_2 = 822 ± 115 s. Conditions: strand concentrations = 6.7 μM in 10 mM Bu_4AmP, 1 mM EDTA, pH 7.0, 25 °C.

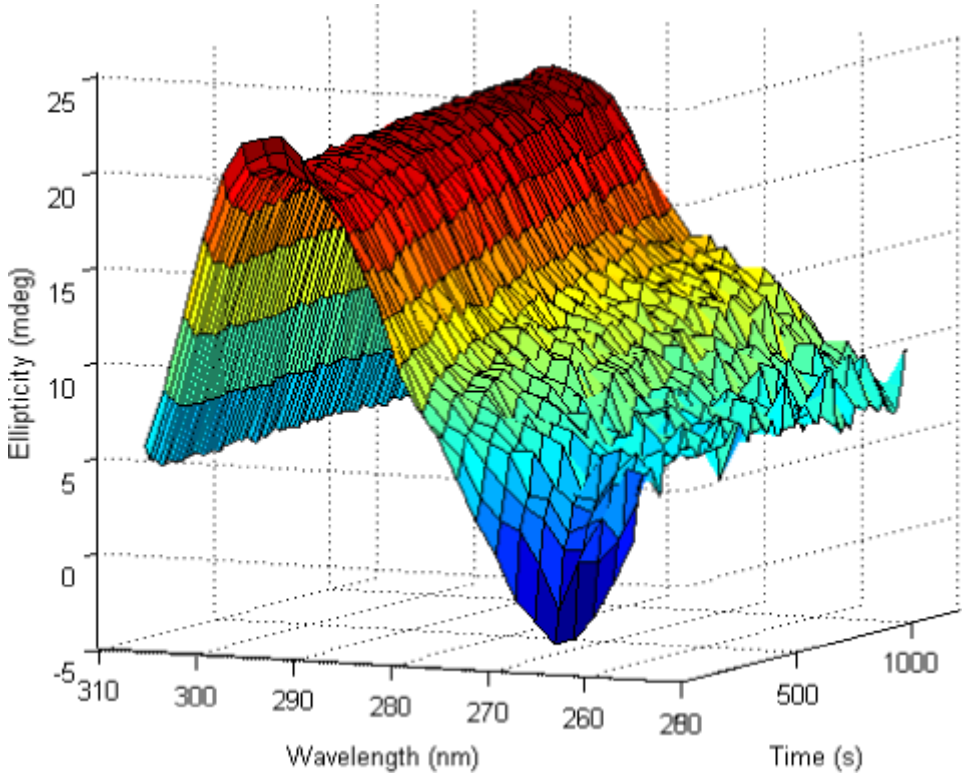

Figure 7.

Three-dimensional plot illustrating time-dependent changes in the CD spectrum associated with the replacement of Na^+ by K^+ in the basket form. Conditions: strand concentration = 6.7 μM in 10 mM Bu_4AmP, 1 mM EDTA, pH 7.0, 25 °C. Initial [NaCl] = 30 mM and the final [KCl] = 50 mM.

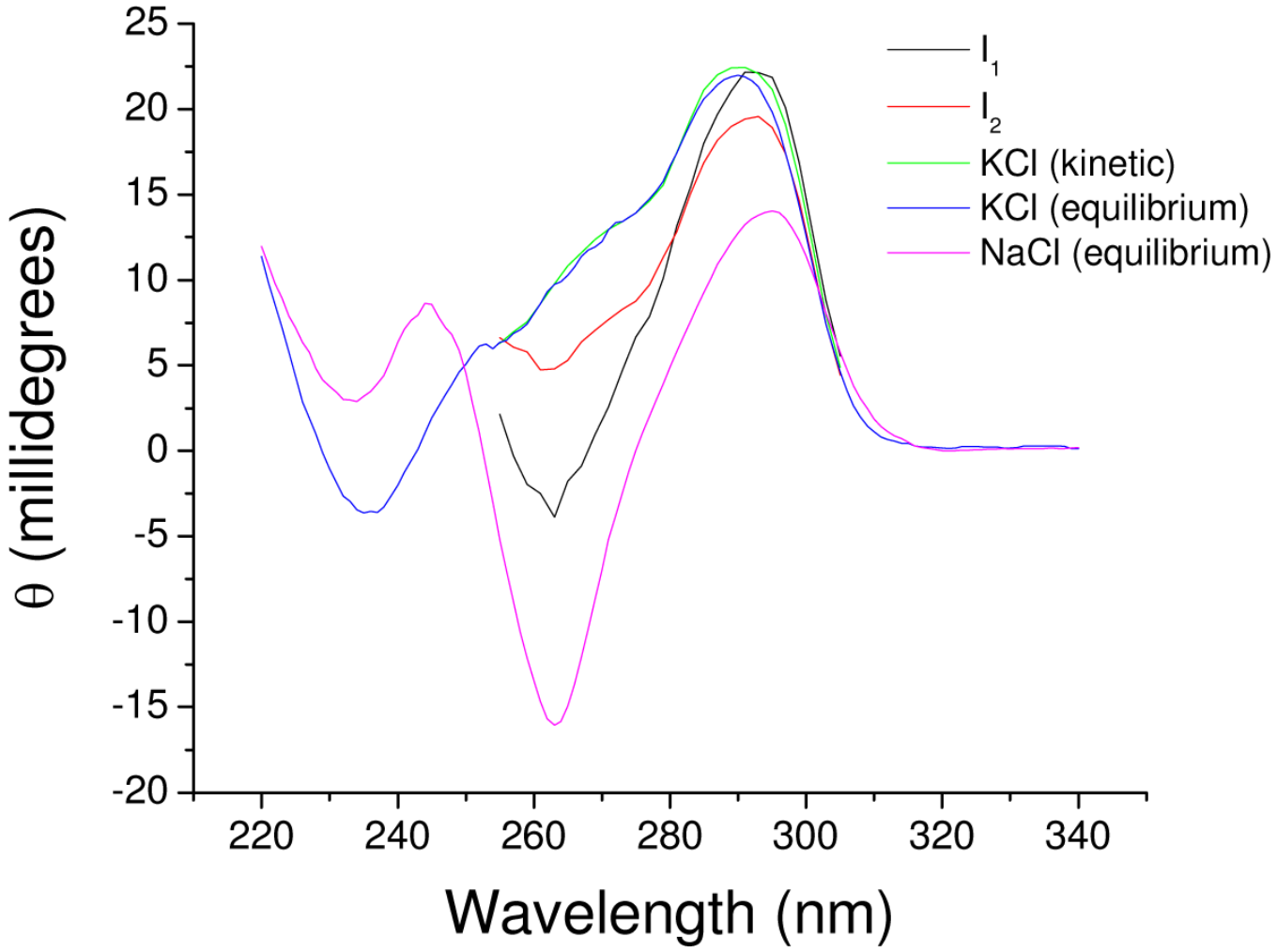

Figure 8.
Comparison of equilibrium CD spectrum of the Na^+ basket form and the K^+-hybrid form with the CD spectra of kinetic intermediates in the Na^+-K^+ exchange reaction. The CD spectra of the intermediates were derived by SVD analysis and fitting the kinetic data matrix to the integrated rate equations corresponding to Scheme 1 using Specfit/32.

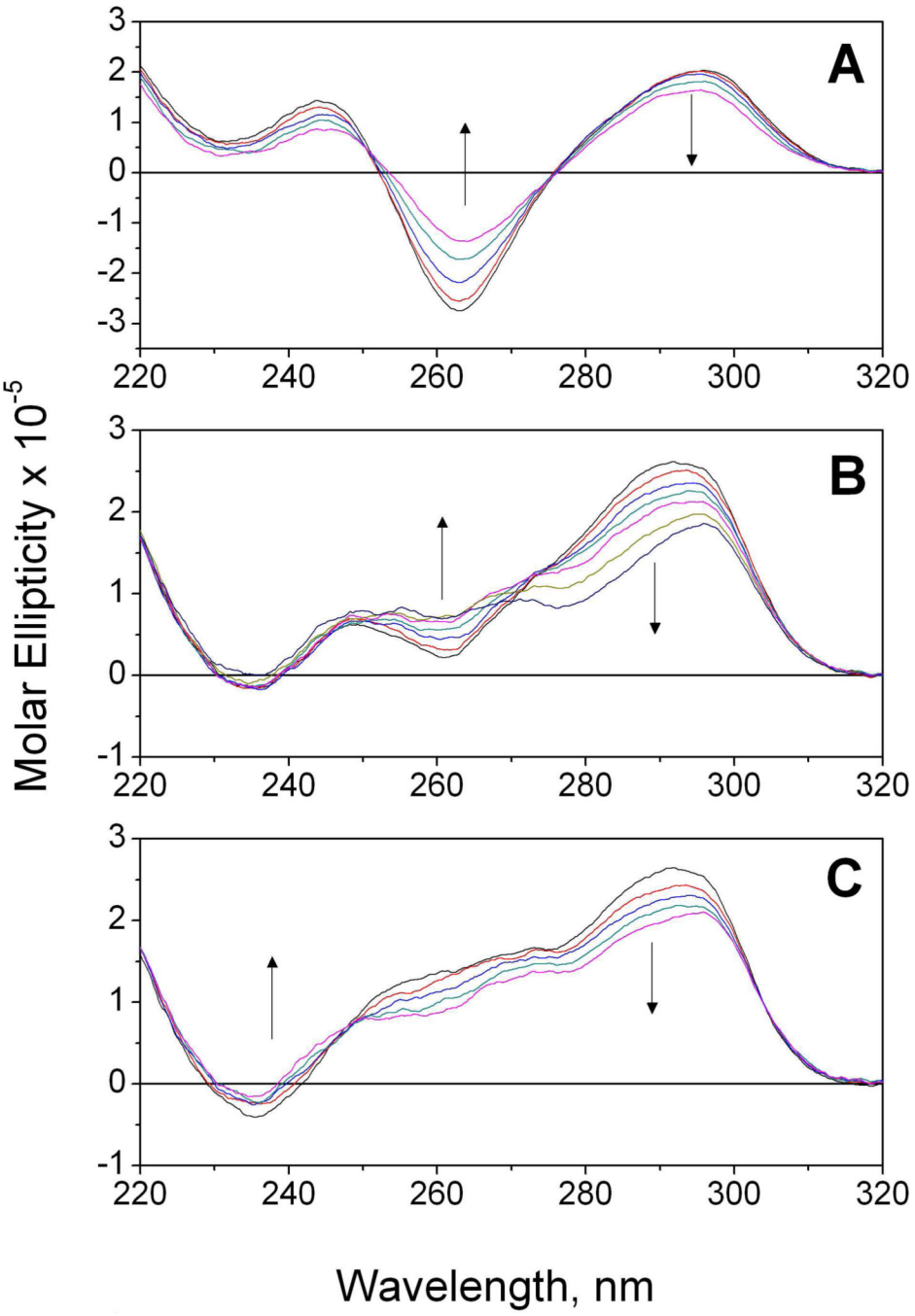

Figure 9.

Conversion of the quadruplex basket form to a hybrid form by TmPyP4. (A) Titration of the Na^+ basket form with TmPyP4. The molar ratios of added ligand range from 0 to 2; the quadruplex concentration was 2 M (strands). (B) Titration of a quadruplex solution of mole fraction sodium of 0.84 containing an equilibrium mixture of basket and hybrid forms with TmPyP4. The molar ratios of added ligand range from 0 to 4; the quadruplex concentration was 2 M (strands). (C). Titration of the K^+ hybrid quadruplex form with TmPyP4. The molar ratios of added ligand range from 0 to 2; the quadruplex concentration was 2 M (strands).

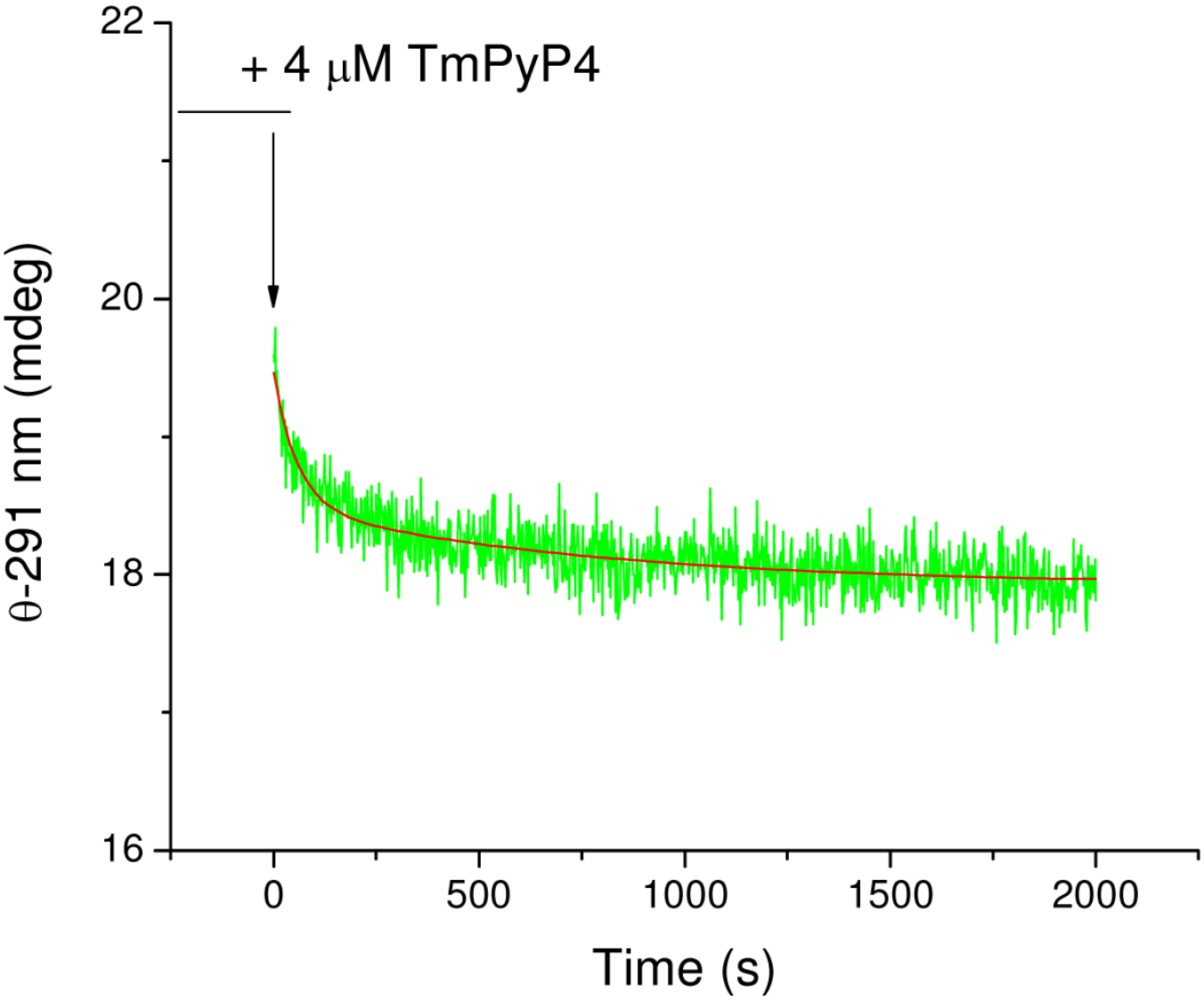

Figure 10.

Kinetics of basket to hybrid structural change induced by binding TmPyP4. The figure shows the change in ellipticity at 291 nm subsequent to mixing with TmPyP4 to give a final porphyrin concentration of 4 μM. The horizontal bar shows the starting ellipticity just before addition of the porphyrin. The vertical arrow shows the rapid decrease in ellipticity that occurs during the mixing time that is followed by a slower biphasic decrease in ellipticity. Conditions: 10 mM Bu_4AmP, 1 mM EDTA, 30 mM NaCl, 5.7 mM KCl, 7 μM oligonucleotide. The green line shows the fit of the data to two exponentials. The optimized relaxation times are τ_1 = 56.6 ± 8.2 s and τ_2 = 742 ± 142 s.

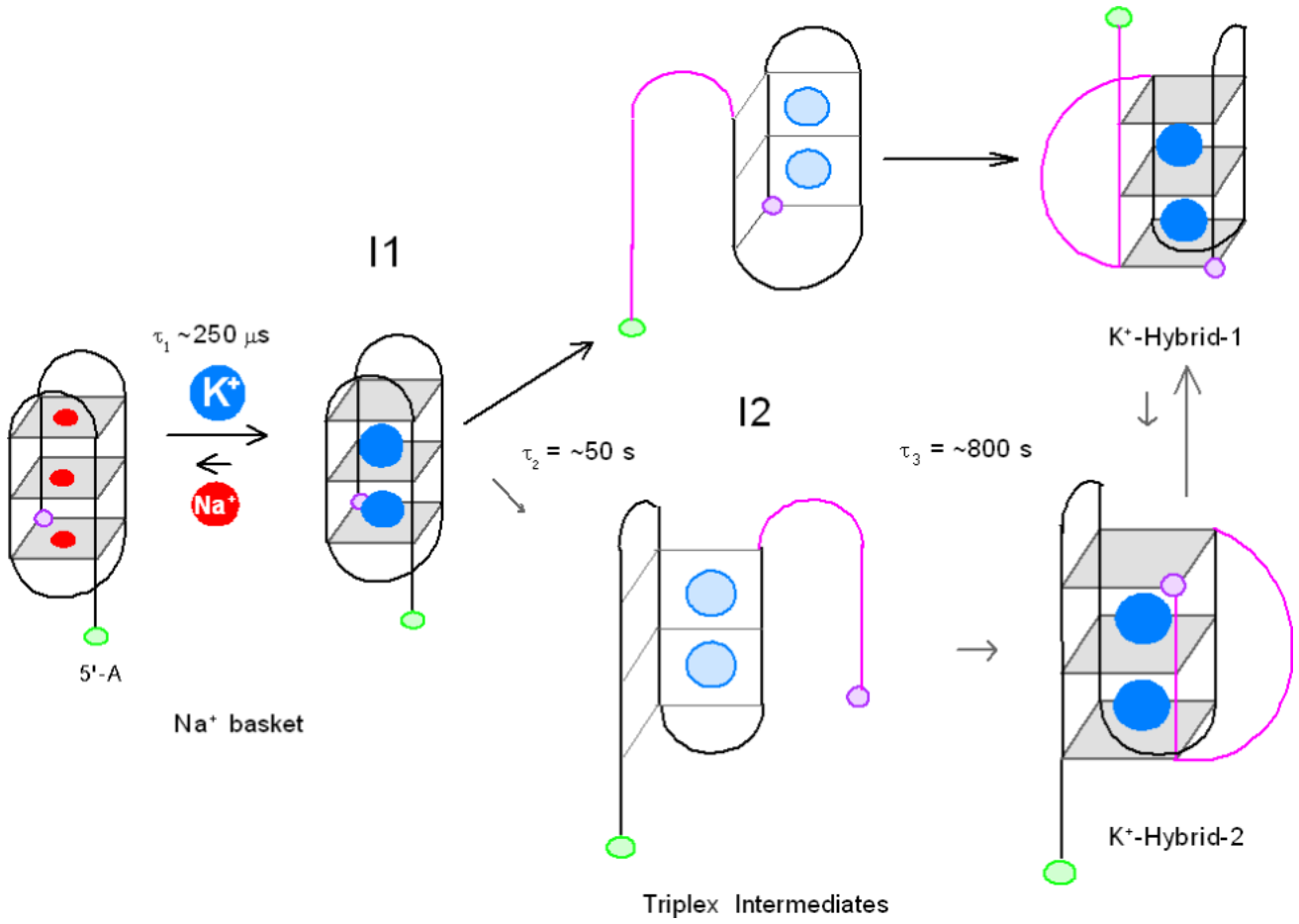

Figure 11.
Cartoon illustrating possible pathway suggested by the kinetic data for conversion of the Na^+-basket to a mixture of hybrid-1 and hybrid-2 forms in K^+. See text for details.

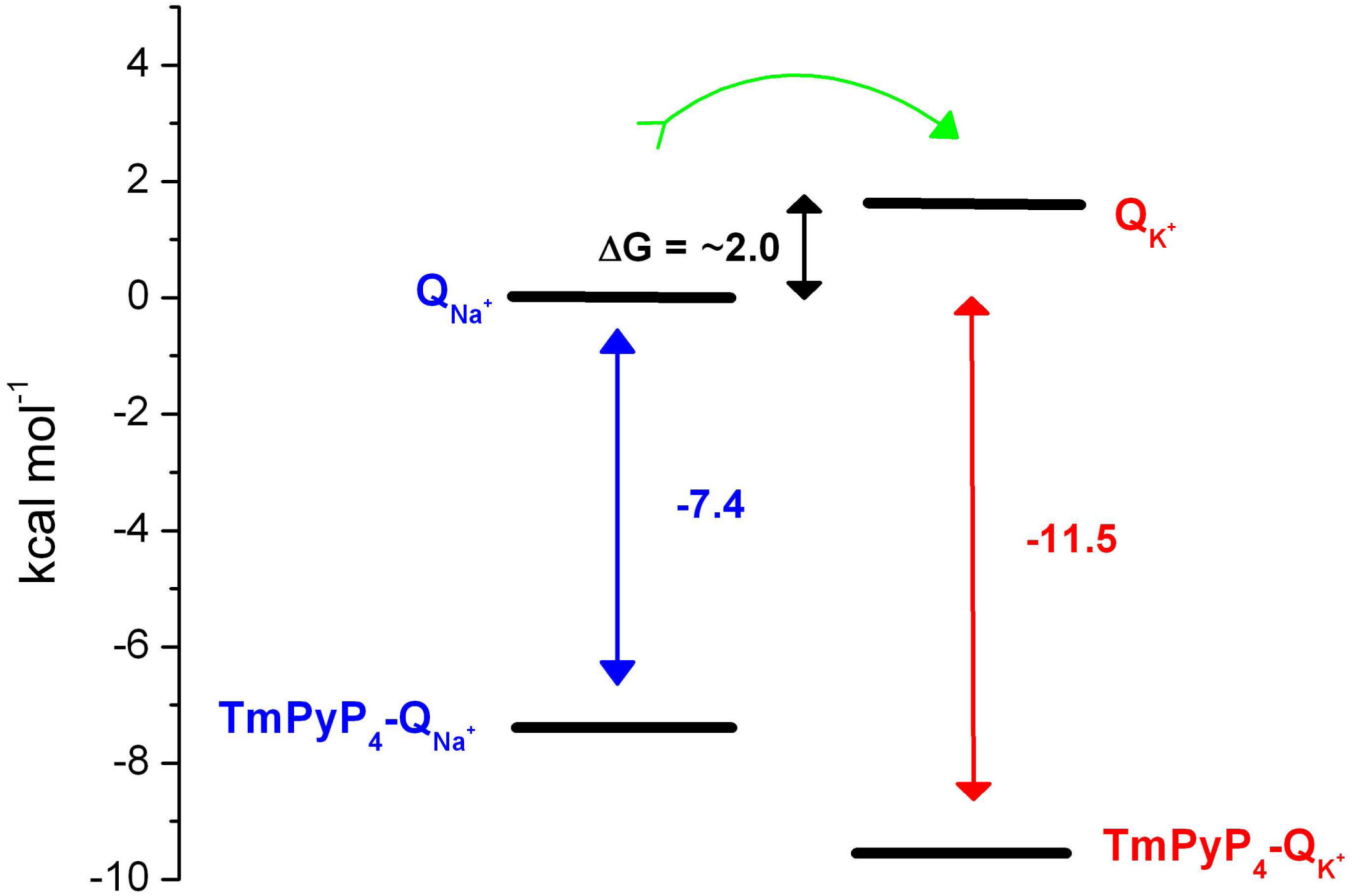

Figure 12.
Tentative energy balance for the TmPyP4 induced conversion of the quadruplex basket form to the hybrid form.